

# Solitons in $\alpha$ -helical proteins

L. Brizhik, and A. Eremko<sup>y</sup>

Bogolyubov Institute for Theoretical Physics, 03143 Kyiv, Ukraine

B. Piette<sup>z</sup> and W. Zakrzewski<sup>x</sup>

Department of Mathematical Sciences, University of Durham,  
Durham DH1 3LE, UK

## Abstract

We investigate some aspects of the soliton dynamics in an  $\alpha$ -helical protein macromolecule within the steric Davydov-Scott model. Our main objective is to elucidate the important role of the helical symmetry in the formation, stability and dynamical properties of Davydov's solitons in an  $\alpha$ -helix. We show, analytically and numerically, that the corresponding system of nonlinear equations admits several types of stationary soliton solutions and that solitons which preserve helical symmetry are dynamically unstable: once formed, they decay rapidly when they propagate. On the other hand, the soliton which spontaneously breaks the local translational and helical symmetries possess the lowest energy and is a robust localized entity. We also demonstrate that this soliton is the result of an hybridization of the quasiparticle states from the two lowest degenerate bands and has an inner structure which can be described as a modulated multi-hump amplitude distribution of excitations on individual spines. The complex and composite structure of the soliton manifests itself distinctly when the soliton is moving and some interspine oscillations take place. Such a soliton structure and the interspine oscillations have previously been observed numerically in [A. C. Scott, Phys.Rev. A 26 578 (1982)]. Here we argue that the solitons studied by A. Scott, are hybrid solitons and that the oscillations arise due to the helical symmetry of the system and result from the motion of the soliton along the  $\alpha$ -helix. The frequency of the interspine oscillations is shown to be proportional to the soliton velocity.

## 1 Introduction

In the 1970s Davydov [1] proposed a nonlinear mechanism for the storage and transfer of vibrational energy (intrapeptide vibration Amid-I) in  $\alpha$ -helical proteins. As a result of the interaction of high-frequency Amid-I vibrations (vibrations of double C=O bond of peptide groups) with the low-frequency acoustic vibrations of the protein, a self-trapping of the Amid-I vibration takes place. This idea has attracted a lot of interest, which has increased even further after the appearance of a paper [2] in which Davydov and Klisukha demonstrated that the corresponding system of equations for a molecular chain admits, in the continuum approximation, a solitonic solution. This solution describes a self-trapped quasiparticle (a lump of vibrational

---

<sup>e</sup>m ail address: brizhik@bitp.kiev.ua

<sup>y</sup>e-m ail address: eremko@bitp.kiev.ua

<sup>z</sup>e-m ail address: B.M.A.G.Piette@durham.ac.uk

<sup>x</sup>e-m ail address: W.J.Zakrzewski@durham.ac.uk

Amid-I energy) that propagates at constant velocity and is accompanied by a self-consistent chain deformation [3].

Since then, various properties of such one-dimensional polaron-like self-trapped states have been studied in detail both analytically and numerically (see, e.g., [4, 6, 5]). Dynamical properties of Davydov solitons and their formation, given various initial conditions of the chain, have been investigated in discrete chains and in continuum models. Most of these results have been obtained for a single chain. Often they have involved numerical values of the parameters that are characteristic of real proteins; thus very often these results have been discussed in the context of an  $\alpha$ -helix. In reality, however, real helices contain three strands, each of which, contains periodically placed peptide groups connected by hydrogen bonds. A three-strand model for an  $\alpha$ -helix was proposed in [7], where the stationary states were first studied. This model represents an  $\alpha$ -helix as a three-strand structure with three peptide groups per cell in a plane perpendicular to the protein axis. Soon afterwards the properties of such soliton states were studied analytically in [8, 9] and numerically in [10, 11].

This model does not include a helical structure of proteins, and so afterwards the model was improved in [12, 13]. In [13] the soliton solutions which do not break the chiral symmetry were found analytically. So far, the most complete numerical study of the problem has been presented by Scott in [12], where the formation of a soliton in a linear chain of a finite length had been investigated using the initial excitation of a certain form localised on two of the three peptide groups at the end of the chain. Scott showed there that, under such conditions, a soliton can be formed and that this soliton propagates along the protein with a constant velocity. It has turned out that such a soliton has an inner structure and that some interchain oscillations of energy take place. These oscillations were compared by Scott with the lines in experimentally measured Raman spectra of living cells (see also [14]). Let us add here also that in this numerical modelling only one type of initial excitation was used, and, as a result, only one value of the velocity of the soliton of a given symmetry was obtained. However, there are several features which suggest that this picture is oversimplified. In fact, we expect the dynamics to contain some oscillatory features. This is due to the discrete nature of the chain and it can also be related to the helical symmetry of the protein and the symmetry of the initial excitation.

The aim of the present paper is to study the soliton states in an  $\alpha$ -helix, to investigate their properties and their stability and to look at the dependence of the internal soliton vibrations on the velocity of the soliton propagation. In Section 2 a general description of the model is given. In Section 3 the elementary excitations of the helix are presented. In Section 4 we describe the results of our analytical studies of soliton states in the adiabatic approximation while the results of our numerical modelling are presented in Section 5. In Section 6 we discuss the applicability of the adiabatic approximation and in Conclusions we make further comments on the physical relevance of our results.

## 2 The general model

Protein macromolecules are long nonbranched polymer chains which are formed as a result of polymerization of amino acids. Amino acid residues in such polymer chains are connected by the peptide bonds in which four atoms (O C N H) form the peptide group and two  $\alpha$ -carbon atoms of the residues are placed in one plane. So the backbone of such a polypeptide chain can be described as a set of comparably rigid planes divided by methylene groups ( $-\text{CHR}-$ ). Because peptide groups (PGs) are bonded with methylene groups by ordinary bonds, a free rotation of PG planes

around these bonds is possible. Due to such rotations, a polypeptide chain can take different spatial configurations. Thus in particular, it can be rolled into a helix. Such a configuration of the polypeptide chain is stabilized by the intrachain hydrogen bonds which are formed between a hydrogen atom of a PG and an oxygen atom of the fourth group along the chain. Such a helical structure, called  $\alpha$ -helix, has 3.6 peptide groups per turn. Thus, the equilibrium positions of the repeated units (PG) in an  $\alpha$ -helix are determined by the radius-vectors

$$\mathbf{R}_1^{(0)} = r \mathbf{e}_x \cos\left(\frac{2\pi l}{3.6}\right) + \mathbf{e}_y \sin\left(\frac{2\pi l}{3.6}\right) + \mathbf{e}_z \frac{a l}{3.6} \quad (1)$$

where  $\mathbf{e}_i$  ( $i = x, y, z$ ) are unit vectors along coordinate axes,  $a$  is a period of the helix,  $r$  is its radius, and  $l$  is an integer labeling each group along the polypeptide chain. The nearest neighbours (sites  $l$  and  $l+1$ ) along the chain are bound by rigid valence bonds and each  $l$ -th group in a helix is bound with  $(l+3)$ -th groups by soft hydrogen bonds forming three spines along the helix.

The three spines along the  $\alpha$ -helix are formed by units with numbers:

$$l_1 = 3n; \quad l_2 = 3n+1; \quad l_3 = 3n+2; \quad (2)$$

or we can write

$$l = 3n + (j-1) \quad (3)$$

where  $j = 1, 2, 3$  and  $n$  runs from 1 to  $N$  with  $N$  being the number of PGs in a hydrogen bond strand.

Thus, for the enumeration of PGs in an  $\alpha$ -helix, we can use the two numbers  $j$  and  $n$  where  $j$ , a cyclic index modulo 3, indicates the spine of the hydrogen bond, and  $n$  enumerates PG in a spine or elementary cells of three PGs from different spines. We can use a different numbering of the cyclic index:  $j^0 = j-1 = 0, 1, 2$ ; or  $j^0 = j-1 = 0, 1, 2$ , or  $j = 1, 2, 3$ .

Introducing a double index  $f, j, n$ , instead of the single number  $l$ , the equilibrium positions of PGs in an  $\alpha$ -helix (1) can be rewritten as

$$\mathbf{R}_{j,n}^{(0)} = r \mathbf{e}_x \cos\left(\frac{2\pi n}{3.6} - j\right) + \mathbf{e}_y \sin\left(\frac{2\pi n}{3.6} - j\right) + \mathbf{e}_z \left(\frac{5an}{6} + j\right); \quad (4)$$

where  $j = \frac{2\pi}{3.6} j^0$  and  $j = \frac{a j^0}{3.6}$ . The spines of hydrogen bonds in an  $\alpha$ -helix are also rolled into a helix of length  $5a$  with 6 PGs per turn.

Due to the softness of hydrogen bonds, PGs can be displaced and their positions in an  $\alpha$ -helix are

$$\mathbf{R}_{j,n} = \mathbf{R}_{j,n}^{(0)} + \mathbf{u}_{j,n} \quad (5)$$

where  $\mathbf{u}_n$  are the displacements of the peptide groups from their equilibrium positions (4).

The potential energy of displacements depends on the distance between the groups and so we can perform the approximation of using only the nearest neighbours interaction. The nearest neighbours along the polypeptide chain are bound together by rigid valence bonds, much more rigid than the hydrogen bond. We can thus assume that the distances between  $l$ -th and  $(l+1)$ -th groups are fixed while the potential energy of displacements is determined only by the variation of the hydrogen bond length and, in an harmonic approximation, it can be written as

$$V = \sum_{j,n} [V(R_{j,n;j,n+1}) - V(R_0)] = \sum_{j,n} \frac{1}{2} w_H (R_{j,n;j,n+1} - R_0)^2; \quad (6)$$

where  $w_H$  is the elasticity of the hydrogen bond. In (6),

$$R_0 = R_{j_m, j_{m-1}}^{(0)} = \mathcal{R}_{j_m}^{(0)} - \mathcal{R}_{j_{m-1}}^{(0)} j = \frac{q}{(2r \sin(\frac{\pi}{6}))^2 + (5a/6)^2}; \quad (7)$$

is the equilibrium length of the hydrogen bond, and

$$R_{j_m, j_{m-1}} = \mathcal{R}_{j_m} - \mathcal{R}_{j_{m-1}} j - R_0 = \frac{(\mathcal{R}_{j_m} - \mathcal{R}_{j_{m-1}})(u_{j_m} - u_{j_{m-1}})}{R_0} \quad (8)$$

are its changes due to the small displacements. The total energy of the displacements is the sum of the potential energy (6) and the kinetic energy which is given by the relation

$$T = \sum_{j_m} \frac{1}{2} M \dot{u}_{j_m}^2; \quad (9)$$

where  $M$  is the mass of a PG and  $\dot{u}_{j_m} = \frac{du_{j_m}}{dt}$  are the velocities of the displacements.

Due to the assumption that the valence bonds are sufficiently rigid and that the distances between the  $l$ -th and  $(l-1)$ -th groups are fixed, the three components of the PG displacement are not independent. In fact, we have two conditions which correspond to the assumption that the distances between each  $l$ -th PG and its two neighbours,  $l-1$  and  $l+1$ , are fixed. For small displacements this means that the displacement  $u_1$  of the  $l$ -th PG is orthogonal to the vectors connecting the  $l$ -th and the  $(l-1)$ -th groups:

$$u_1 \cdot (R_l - R_{l-1}) = 0; \quad u_1 \cdot (R_l - R_{l+1}) = 0; \quad (10)$$

Let us represent the vector  $u_1$  using three orthogonal unit vectors  $e_1^{(r)}$ ,  $e_1^{(t)}$  and  $e_z$ :

$$u_1 = e_1^{(r)} u_1^{(r)} + e_1^{(t)} u_1^{(t)} + e_z u_1^k; \quad (11)$$

where  $e_z u_1^k = u_1^k$  is the longitudinal, (along the  $z$ -helix axis) component of the displacement. The transversal component  $u_1^{(t)} = e_1^{(r)} u_1^{(r)} + e_1^{(t)} u_1^{(t)}$  is represented through the radial and tangential components relative to the axis. Here

$$e_1^{(r)} = e_x \cos(\frac{2\pi}{3\phi}) + e_y \sin(\frac{2\pi}{3\phi}); \quad e_1^{(t)} = -e_x \sin(\frac{2\pi}{3\phi}) + e_y \cos(\frac{2\pi}{3\phi}); \quad (12)$$

In this case condition (10) takes the form

$$\frac{a}{3\phi} u_1^{(ij)} + 2r \sin^2(\frac{\pi}{3\phi}) u_1^{(r)} + r \sin(\frac{2\pi}{3\phi}) u_1^{(t)} = 0; \quad \frac{a}{3\phi} u_1^{(ij)} - 2r \sin^2(\frac{\pi}{3\phi}) u_1^{(r)} + r \sin(\frac{2\pi}{3\phi}) u_1^{(t)} = 0; \quad (13)$$

From these equations it is easy to find that

$$u_1^{(r)} = 0; \quad u_1^{(t)} = \frac{a}{3\phi r \sin(2\pi/3\phi)} u_1^k; \quad (14)$$

Thus, there is only one independent degree of freedom of the PG displacement and the vector of the displacement  $u_{j_m}$  can be represented as

$$u_{j_m} = e_{j_m} u_{j_m} \quad (15)$$

where

$$e_{j_m} = \frac{1}{C} \left[ a \sin(\frac{2\pi}{6} j) e_x + \cos(\frac{2\pi}{6} j) e_y + 3\phi r \sin(\frac{2\pi}{3\phi}) e_z \right]; \quad (16)$$

$$C = \frac{s}{a^2 + 3 \sin^2(\frac{2}{3})r} \quad (17)$$

is the unit vector which determines the direction of small displacements without changing of the valence bond length and  $u_{jm}$  is the amplitude of the displacements.

Taking into account this expression, we obtain the following expression for the change of the hydrogen bond length (8)

$$R_{jm;jm-1} = (u_{jm} - u_{jm-1}); \quad (18)$$

where

$$= \frac{ra}{CR_0} \sin \frac{2}{3} + 3 \sin \frac{2}{3} : \quad (19)$$

Thus, the potential energy (6) is

$$V = \sum_{jm} \frac{1}{2} w (u_{jm} - u_{jm-1})^2; \quad (20)$$

where  $w = 2w_H$  is an effective elasticity coefficient.

Therefore, the Hamiltonian of the  $\alpha$ -helix vibrations can be rewritten in the form

$$H_v = \sum_{jm} \left( \frac{p_{jm}^2}{2M} + \frac{1}{2} w (u_{jm} - u_{jm-1})^2 \right) \quad (21)$$

where  $p_{jm}$  are the momentum operators that are canonically conjugate to the operators of the PG's displacement  $u_{jm}$ .

We now focus on the Hamiltonian for the quasiparticle. The states of the Amid-I vibrations of the peptide groups (or extra electron(s)) in the tight binding approximation are described by the Hamiltonian

$$H_e = \sum_l E_0 A_l^+ A_l + \sum_m L_m (A_l^+ A_{l-m} + A_{l-m}^+ A_l) \quad (22)$$

where  $l$  and  $m$  run over the  $3N$  values along the polypeptide chain. Here  $A_l^+$  and  $A_l$  are, respectively, the creation and annihilation operators of the quasiparticle at the  $l$ -th site of the chain;  $L_m$  are the matrix elements of the excitation exchange between sites  $l$  and  $l-m$ . The matrix elements  $L_m$  with  $m$  being a multiple of 3 describe the energy exchange between the PGs of the same spine while the others describe the excitation exchange between the spines. For Amid-I excitations in an  $\alpha$ -helix the numerical values of  $L_m$  decrease with increasing  $m$ . In what follows we will take into account only two the most important terms:  $L_1 = L$  which describes the interspine exchange, and  $L_3 = J$  which describes the intraspine one. The signs of the corresponding matrix elements are chosen in such a way that they correspond to the polypeptide  $\alpha$ -helix [15, 5]

Using the double index  $fj;ng$ :  $A_l = A_{jm}$  we can rewrite (22) as

$$H_e = \sum_n \sum_j \left[ E_0 A_{jm}^+ A_{jm} - J A_{jm}^+ (A_{j,m+1} + A_{j,m-1}) + L A_{1,m}^+ (A_{3,m-1} + A_{2,m}) + A_{2,m}^+ (A_{1,m} + A_{3,m}) + A_{3,m}^+ (A_{2,m} + A_{1,m+1}) \right] \quad (23)$$

where  $n$  runs from 1 to  $N$  and enumerates the cells on each of the 3 strands.

We now consider the Hamiltonian for the interaction of a quasiparticle with the chain distortion. Due to the softness of the hydrogen bonds and the stiffness of the valence bonds, the distance between the  $n$ -th and  $(n+3)$ -th group changes only under distortions of the  $\alpha$ -helix. So, taking into account the on-site deformation potential only (the dependence of  $J$  on the distance between the groups is not so essential for an  $\alpha$ -helix [5]), we can write the interaction Hamiltonian in the form

$$H_{\text{int}} = \sum_{jm} (u_{jm+1} - u_{jm-1}) A_{jm}^+ A_{jm} : \quad (24)$$

where  $u$  is a constant parameterising the strength of the exciton (electron)-phonon interaction.

The total Hamiltonian

$$H = H_e + H_v + H_{\text{int}} \quad (25)$$

where  $H_e$ ,  $H_v$ , and  $H_{\text{int}}$  are given by (23), (21), and (24), respectively, describes the dynamics of a molecular helical chain in which the equilibrium positions of its units (PGs) are given by the radius-vectors

$$\mathbf{R}_{jm}^{(0)} = r \mathbf{e}_x \cos(\frac{2}{3}j) + \mathbf{e}_y \sin(\frac{2}{3}j) + \mathbf{e}_z a(n + \frac{j}{3}) \quad (26)$$

where  $j$  is a cyclic index (of modulus 3), which enumerates the three spines along the  $z$  axes, and  $n$  is the position index of an elementary cell within the three strands. Equation (26) describes a molecular chain which is rolled into a helix with three units per turn of the helix. We can consider such a molecular chain as a model of the  $\alpha$ -helical protein. In this case we can neglect the rolling of the hydrogen bonds into a superhelix.

### 3 Elementary excitations in an $\alpha$ -helix

The quasiparticle Hamiltonian (23) can be diagonalized by the following unitary transformation

$$A_{jm} = \frac{1}{\sqrt{N}} \sum_{\mathbf{k}} e^{i\mathbf{k}m} v_{j,\mathbf{k}}(\mathbf{k}) B_{\mathbf{k}}; \quad v_{j,\mathbf{k}}(\mathbf{k}) = \frac{1}{\sqrt{3}} e^{i(\frac{\mathbf{k}}{3})j}; \quad (27)$$

where the wave number  $\mathbf{k}$  and the band index  $j$  are given by

$$\mathbf{k} = \frac{2}{N} \mathbf{l}; \quad \mathbf{l} = 0; 1; \dots; \frac{N-1}{2}; \quad \frac{2}{N} \mathbf{l} = \frac{2}{3} \mathbf{l}; \quad \mathbf{l} = 0; 1; \dots; \frac{N-1}{2}; \quad (28)$$

Under transformation (27), the Hamiltonian (23) transforms into

$$H_e = \sum_{\mathbf{k}} E(\mathbf{k}) B_{\mathbf{k}}^+ B_{\mathbf{k}} \quad (29)$$

where the energy dispersion in the three bands ( $j = 0; \frac{2}{3}$ ) is given by

$$E(\mathbf{k}) = E_0 - 2J \cos(\mathbf{k}) + 2L \cos \frac{\mathbf{k}}{3} + \quad (30)$$

or, in explicit form, by

$$\begin{aligned} E_0(\mathbf{k}) &= E_0 - 2J \cos(\mathbf{k}) + 2L \cos \frac{\mathbf{k}}{3}; \\ E(\mathbf{k}) &= E_0 - 2J \cos(\mathbf{k}) - L \cos \frac{\mathbf{k}}{3} - \frac{P}{3L} \sin \frac{\mathbf{k}}{3}; \end{aligned} \quad (31)$$

The Hamiltonian  $H_v$  (21) describes independent oscillations of the PG in the spines of H-bonds in an  $\alpha$ -helix.

Next, we perform a unitary transformation of the lattice variables:

$$u_{jn} = \frac{1}{\sqrt{N}} \sum_q e^{iqn} \frac{\hbar}{2M \omega_q} \left( a_{jq} + a_{jq}^\dagger \right) \quad (32)$$

$$p_{jn} = \frac{i}{\sqrt{N}} \sum_q e^{iqn} \frac{\hbar M \omega_q}{2} \left( a_{jq} - a_{jq}^\dagger \right); \quad (33)$$

where  $a_{jq}^\dagger$  and  $a_{jq}$  are the operators of creation and annihilation of acoustic phonons with wavenumber  $q$  and frequency

$$\omega_q = 2 a_j \sin \frac{q}{2}; \quad a_j = \frac{r}{M}; \quad (34)$$

As it is convenient to describe the lattice oscillations in the helical symmetry representation that we have introduced for the description of excitons, we define the operators  $b_q$  as

$$a_{jq} = \sum_j v_j(q) b_q; \quad (35)$$

where the  $v_j(q)$  were given in the description of the excitons (27). In this formulation, the displacement operator is given by

$$u_{jn} = \frac{1}{\sqrt{N}} \sum_q e^{iqn} v_j(q) \frac{\hbar}{2M \omega_q} \left( b_q + b_q^\dagger \right) \quad (36)$$

and the Hamiltonian  $H_v$  (21) takes the form

$$H_v = \sum_q \hbar \omega_q \left( b_q^\dagger b_q + \frac{1}{2} \right); \quad (37)$$

Thus, the elementary excitations are given by the phonons which correspond to the deformational oscillations of the lattice, and the excitons which describe the internal Amid excitations of the PG. As an elementary cell contains 3 PGs, the spectrum consists of three exciton bands which correspond to the Davydov splitting. This band structure is shown in Fig. 1 for  $L = 12.4 \text{ cm}^{-1}$  and  $J = 7.8 \text{ cm}^{-1}$ , which correspond to the  $\alpha$ -helix values.

Finally, we rewrite the interaction Hamiltonian  $H_{int}$  (24) as

$$H_{int} = \frac{1}{3N} \sum_{kq} f(q) B_{+k+q}^\dagger B_{-k} b_q + (q) B_{-k}^\dagger B_{+k+q} b_q^\dagger; \quad (38)$$

where

$$f(q) = i \frac{2\hbar}{M \omega_q} \frac{1}{2} \sin(q); \quad (39)$$

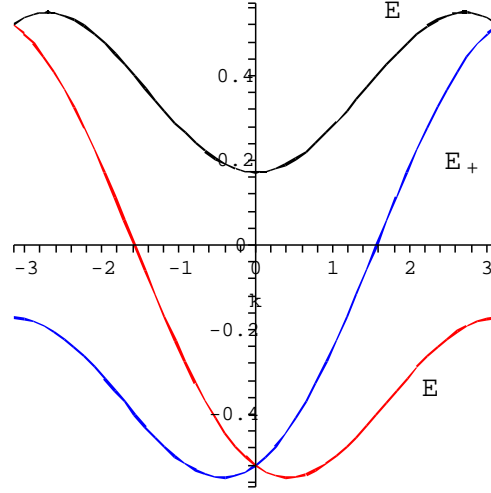


Figure 1: The three energy bands (31) for  $J = 7.8 \text{ cm}^{-1}$  and  $L = 12.4 \text{ cm}^{-1}$

#### 4 Equations in the adiabatic approximation

In the adiabatic approximation the wavefunction of the system with one quasiparticle is represented as

$$|j(t)\rangle = U(t) |j_e(t)\rangle; \quad (40)$$

where  $U(t)$  is the unitary operator of the coherent molecule displacements

$$U(t) = \exp \left( \sum_{\alpha} (b_{\alpha}^{\dagger}(t) b_{\alpha}^y - b_{\alpha}(t) b_{\alpha}^{\dagger}) \right); \quad (41)$$

$$|j_e(t)\rangle = \sum_{\mathbf{k}} b_{\mathbf{k}}(t) B_{\mathbf{k}}^y |j\rangle; \quad (42)$$

with functions  $b_{\mathbf{k}}(t)$  that satisfy the normalisation condition:

$$\sum_{\mathbf{k}} |b_{\mathbf{k}}(t)|^2 = 1; \quad (43)$$

The coefficients  $b_{\alpha}(t)$  in (41) are, at this stage, arbitrary functions which will be determined below.

In the adiabatic approximation the equations for  $b_{\mathbf{k}}(t)$  and  $b_{\alpha}(t)$  can be obtained either directly from the time dependant Schrodinger equation or as Hamilton equations for the generalized variables  $b_{\mathbf{k}}(t)$ ,  $b_{\alpha}(t)$  and their canonically conjugated momenta  $(i\hbar) \dot{b}_{\mathbf{k}}(t)$  and  $(i\hbar) \dot{b}_{\alpha}(t)$  by considering

$$\begin{aligned} H = \hbar \langle j | j \rangle = & \sum_{\mathbf{k}} E(\mathbf{k}) b_{\mathbf{k}}^{\dagger} b_{\mathbf{k}} + \sum_{\alpha} \hbar \omega_{\alpha} (b_{\alpha}^{\dagger} b_{\alpha} + \frac{1}{2}) \\ & + \frac{1}{3N} \sum_{\mathbf{k}; \alpha} (q_{\alpha} + b_{\mathbf{k}+\alpha} b_{\mathbf{k}} (b_{\alpha}^{\dagger} + b_{\alpha})) \end{aligned} \quad (44)$$



as a Hamilton functional. The equations are thus given by

$$i\hbar \frac{d}{dt} \psi_k(t) = E(k) \psi_k(t) + \sum_{q_j} \frac{2i \sin q_j}{3NM} Q(q_j; t) \psi_{k-q_j}(t); \quad (45)$$

$$i\hbar \frac{d}{dt} Q(q; t) = \hbar^2 q^2 Q(q; t) + \frac{1}{3NM} \sum_{k_j} (q) \psi_{k_j} + \psi_{k_j+q}; \quad (46)$$

In the first equation,  $Q(q; t)$  is given by

$$Q(q; t) = \frac{\hbar}{2! q} \psi_{q/2} + \dots; \quad q: \quad (47)$$

In fact, the equation for  $\psi_{q/2}(t)$  becomes the equation for  $Q(q; t)$  and takes the form:

$$\frac{d^2 Q(q; t)}{dt^2} + \hbar^2 q^2 Q(q; t) = \frac{2i \sin q}{3NM} \sum_{k_j} \psi_{k_j}(t) + \psi_{k_j+q}(t); \quad (48)$$

In these expressions, and in what follows, the index labeling and  $Q$  is defined modulo 3.

Next, we seek the stationary solutions of these equations by requiring that

$$\psi_k(t) = e^{i(\omega(k)t + k z_s(t))} \phi(k); \quad (49)$$

This immediately tells us that

$$Q(k; t) = e^{ik z_s(t)} Q(k); \quad (50)$$

Here the parameter  $z_s(t)$  corresponds to the centre of mass of the excitation.

Substituting this ansatz into our equations, we obtain

$$[\hbar^2 + \hbar V k - E(k)] \phi(k) = \sum_{q_j} \frac{2i \sin q_j}{3NM} Q(q_j) \phi(k - q_j); \quad (51)$$

$$(\hbar^2 q^2 - V^2 q^2) Q(q; t) = \frac{2i \sin k}{3NM} \sum_{k_j} \phi(k_j) + \phi(k_j + q); \quad (52)$$

where  $\omega = \frac{dE}{dk}$  and  $V = \frac{dz_s}{dt}$  is the velocity of the propagation of the excitation measured in units of the lattice constants.

Taking into account (52), we see that (51) is a nonlinear integrodifferential equation. From (51) we see that  $\phi(k)$  has a maximum at the carrying wave number  $k_c$  which corresponds to the minimum of  $\hbar^2 + \hbar V k - E(k)$ , i.e.  $k_c$  and the excitation velocity  $V$  are connected by the relation

$$\hbar V = \left. \frac{dE(k)}{dk} \right|_{k=k_c}; \quad (53)$$

Next, we assume that, in the space representation, the solution is given by a wave packet broad enough so that it is sufficiently narrow in the  $k$  representation. This means that  $\phi(k)$  are essentially nonzero only in a small region of values of  $k$  in the vicinity of  $k_c$ . In this case we can use the following approximation

$$\hbar^2 + \hbar V k - E(k) = \frac{\hbar^2 (k - k_c)^2}{2m}; \quad (54)$$

where

$$= [\hbar + \hbar V k - E(k)]_{k=k_c} ; \quad \frac{\hbar^2}{m} = \frac{d^2 E(k)}{dk^2} \Big|_{k=k_c} : \quad (55)$$

To solve (51), we introduce the position dependent functions

$$\psi(x) = \frac{1}{N} \sum_k e^{i(k - k_c)x} \phi(k) : \quad (56)$$

Note that at  $x = n$  this is a unitary transformation of  $\phi(k)$  to the site representation. Using approximation (54), one can transform (51) into a differential equation for  $\psi(x)$ :

$$\psi(x) + \frac{\hbar^2}{2m} \frac{d^2 \psi(x)}{dx^2} = \sum_k V(x) e^{i(k_c - k_c(x))x} \psi(x) = 0 ; \quad (57)$$

where

$$V(x) = \frac{1}{3MN} \sum_q e^{iqx} Q(q) \sin q : \quad (58)$$

Note also that (57) is only a zero-order approximation of (51) and so it corresponds to the continuum approximation. Only in this approximation the soliton velocity  $V$  and frequency are constant and the soliton centre of mass evolves with time as  $z_s(t) = Vt + z_0$  and  $\phi(t) = \phi_0$ .

Finally note that, when transforming (51) into (57), one has to be careful with the double summation  $\sum_{k,q} \dots$ . The wavenumbers  $k$  and  $q$  are in the first Brillouin zone,  $-\pi < k, q \leq \pi$ , and the wave number  $k - q$  also has to be in this zone. This is the case for small values of  $k$  and  $q$  (normal processes in exciton-phonon interactions). However, when  $k$  and  $q$  are close to the edge of the first Brillouin zone, it is possible that  $|k - q| > \pi$  (Umklapp processes). In this case it is necessary to reduce the wave number  $k - q$  to the first Brillouin zone using the reciprocal lattice wave number  $g = 2\pi/a$ . This does not change the discrete equations due to the periodicity of the functions in the space of reciprocal lattice vectors, but is essential when introducing continuous functions for the analytical investigations. The Umklapp processes lead to the appearance of additional terms in (57) for which the double summations are performed in the regions near the edges of the Brillouin zone where  $|k - q| > \pi$ . The assumption that  $\phi(k)$  and  $Q(q)$  are small in these regions allows us to consider these terms as a perturbation. Here we do not take this perturbation into consideration. A detailed analysis can be found in [19] where it has been shown that allowing Umklapp processes in  $k$  space leads to the appearance of a periodical (with a period of a lattice constant) Peierls-Nabarro potential barrier for the motion of the soliton centre of mass ([16, 17, 18, 19]). As a result, in discrete lattices, the "instantaneous" soliton velocity depends on time and has an oscillatory component with a period

$$T_d = \frac{2}{V_{av}} ; \quad (59)$$

where  $V_{av}$  is the average velocity of the soliton propagation in the chain.

Having found the solutions of (57), we can then use the transformation (27) and, taking into account (49) and (56), write down the probability amplitudes for the distribution of the excitations in an  $n$ -helix:

$$j_n(t) = \frac{1}{N} \sum_k e^{ikn} \psi_j(k) ; \quad \psi_k(t) = \frac{1}{3} e^{i(+V k_c)t + ik_c n + i(+\frac{1}{3}k_c)j} , \quad (n + \frac{1}{3}j - Vt) : \quad (60)$$

From (52) we obtain the explicit expressions for  $Q_0(q)$  at  $\alpha = 0$  and  $\alpha = 3$ , namely:

$$Q_0(q) = \frac{2i \sin q}{(\frac{1}{2}q^2 - V^2 q^2)^{3/2}} \sum_{\mathbf{k}} \mathbf{k} \cdot (\mathbf{k} + \mathbf{q}) e^{i\mathbf{k} \cdot \mathbf{x}} \quad (61)$$

$$Q_+(q) = \frac{2i \sin q}{(\frac{1}{2}q^2 - V^2 q^2)^{3/2}} \sum_{\mathbf{k}} \left[ \epsilon_0(\mathbf{k}) + (\mathbf{k} + \mathbf{q}) + \epsilon_+(\mathbf{k}) - (\mathbf{k} + \mathbf{q}) + \epsilon_-(\mathbf{k}) - \epsilon_0(\mathbf{k} + \mathbf{q}) \right] e^{i\mathbf{k} \cdot \mathbf{x}}; \quad (62)$$

$$Q_-(q) = Q_+(q): \quad (63)$$

Substituting these expressions into (58), we obtain the potentials  $V_0(x)$ . For example,

$$V_0(x) = \frac{1}{N} \sum_{\mathbf{q}, \mathbf{k}} \frac{2 \sin^2 q}{3M (\frac{1}{2}q^2 - V^2 q^2)} e^{i\mathbf{k} \cdot \mathbf{x}} (\mathbf{k}) e^{i(\mathbf{k} + \mathbf{q}) \cdot \mathbf{x}} (\mathbf{k} + \mathbf{q}): \quad (64)$$

We can see from (61) that  $Q_0(q)$  is essentially nonzero only at small values of  $q$ . So we can use the long-wave approximation and write the phonon dispersion relation (34) as  $\epsilon_q \approx \frac{1}{2}q^2$ . In this case  $V_0(x)$  is given by

$$V_0(x) = \frac{2}{3w(1 - v^2)} \sum_{\mathbf{x}} \mathbf{x}^2 \quad (65)$$

where  $v = V/v_a$  is a velocity in units of sound velocity  $v_a$ . Similarly, the potentials  $V_{\pm}(x)$  are quadratic in  $\mathbf{x}$ . Therefore, the system of equations (57) is a system of nonlinear Schrodinger equations (NLSEs).

We observe that equations (57) admit three types of ground state solutions of a soliton type which preserve the helical symmetry of the system. Such solutions describe solitons which are formed by excitons from only one of the three excitonic bands, i.e. only one function  $\psi \neq 0$  for a given  $\mathbf{x}$  is nonzero and the other two  $\psi = 0$  with  $\mathbf{x} \in \mathbb{R}^3$ . In such states, according to (61)–(62), only the total symmetrical distortion of the  $\alpha$ -helix takes place, i.e.  $Q_0(q) \neq 0$  and  $Q_{\pm}(q) = 0$ . Taking into account (65), we note that these types of solitons are described by the NLSE:

$$\psi''(x) + \frac{\hbar^2}{2m} \frac{d^2 \psi}{dx^2} + \frac{2}{3w(1 - v^2)} \sum_{\mathbf{x}} \mathbf{x}^2 \psi^2(x) \psi(x) = 0 \quad (66)$$

together with the normalisation condition (43). Its solution is given by

$$\psi(x) = \frac{1}{2} \frac{1}{\cosh(\frac{x}{\lambda})} \quad (67)$$

with the eigenvalue

$$E = \frac{\hbar^2}{2m}; \quad (68)$$

where

$$\lambda = \frac{m}{3\hbar w(1 - v^2)}; \quad (69)$$

Thus, from (55) we find that

$$\hbar \omega = E(\mathbf{k}_c) - V \mathbf{k}_c \cdot \frac{\hbar^2 \mathbf{k}_c}{2m}; \quad (70)$$

According to (60),

$$\psi_{jm}(t) = \frac{1}{6} \frac{e^{i(n + \frac{1}{3}j)Vt + ik_c(n + \frac{1}{3}j) + i\phi_j}}{\cosh(Vt - \phi_j)} : \quad (71)$$

This excitation is spatially distributed between the chains with the probability components given by:

$$P_{jm}(t) = \frac{1}{3} \left( n + \frac{j}{3} - Vt - \phi_j \right) : \quad (72)$$

Clearly,  $P_j = \sum_n P_{jm} = 1/3$ . For the totally symmetric soliton,  $\phi_j = 0$ , the chains are excited with the same phase, while for the other two cases,  $\phi_j = \pm 2\pi/3$  and the excitations in the spines have the phase shifts  $\pm 2\pi/3$ .

Note that due to the factor  $(1 - v^2)$  in (65) and (69) we see that the soliton velocity  $V$  cannot exceed the sound velocity  $v_a$ . However, there is also a further restriction on the soliton velocity which follows from (53). Unlike for the parabolic law, the energy dispersion in an exciton band shows that  $dE(k)/dk$  has a maximum value. Therefore, (53) has a solution only when  $V$  does not exceed the maximum exciton group velocity  $V_g = (1/\hbar)(dE(k)/dk)_{\max}$  and so, the top speed of the solitons is determined by the lowest of  $v_a$  and  $V_g$ . For example, in a simple chain with  $E(k) = 2J \cos k$ ,  $V_g = 2J/\hbar$ , and with the parameters of the  $\alpha$ -helix,  $v_a > V_g$ .

Below we will consider solitons at low velocities. In this case, from (53), we have

$$k_c = k + \frac{m}{\hbar} V : \quad (73)$$

Here  $k$  determines the bottom of the  $j$ -th exciton band and  $m$  is an effective exciton mass near the band bottom. At low velocities the total energy  $E = H$  of the soliton state is given by

$$E(V) = E(0) + \frac{1}{2} M V^2 : \quad (74)$$

The totally symmetric exciton band has a minimum at  $k_0 = 0$  and, in the long-wave approximation, we have

$$E_0(0) = E_0 - 2J + 2L; \quad m_0 = \frac{9\hbar^2}{2(9J - L)} \quad (75)$$

Therefore, the totally symmetric soliton state is characterized by the width parameter

$$\phi_0 = \frac{3}{w(9J - L)}; \quad (76)$$

the energy

$$E_0(0) = E_0 - 2J + 2L - \frac{4}{3w^2(9J - L)}; \quad (77)$$

and the mass

$$M_0 = m_0 + \frac{8}{3a^2w^2(9J - L)}; \quad (78)$$

The other two of the three soliton states are formed by excitons from the other two bands,  $j = \pm 1$ . Due to the helical symmetry, the bottoms of these bands are determined by the non-zero wavenumbers  $k = \pm k_d$ . For an  $\alpha$ -helix the parameter  $k_d$  is small and can be determined in the long-wave approximation as

$$k_d = \frac{9L}{3(18J + L)} : \quad (79)$$

Thus, for these bands we have

$$E_1(0) = E_1 = E_0 - 2J - L \frac{3L^2}{2(18J + L)}; \quad m_1 = \frac{9h^2}{18J + L} \quad m_1; \quad (80)$$

Therefore, these soliton states are characterized by the width parameter

$$l_1 = \frac{6^2}{w(18J + L)(1 - v^2)}; \quad (81)$$

the total energy at rest

$$E_1(0) = E_0 - 2J - L \frac{3L^2}{2(18J + L)} - \frac{2^4}{3w^2(18J + L)}; \quad (82)$$

and by the soliton mass

$$M_1 = m_1 + \frac{16^4}{3(18J + L)w^2 \frac{2}{a}}; \quad (83)$$

Note that the energies of these three solitons are split from the bottoms of the corresponding energy bands. We should add that the solutions of these soliton states were also found in [13].

The energy levels of the last two solitons are degenerate. However, according to the Jan-Teller theorem, this degeneracy can be broken by the distortions of the chains and a hybridization of these two states can take place. Below we consider such a case when i.e.,  $\epsilon \neq 0$  and  $\epsilon_0 = 0$ .

In this case we find from (57) that  $\psi$  are determined by the system of equations:

$$\psi_+(x) + \frac{h^2}{2m_1} \frac{d^2 \psi_+(x)}{dx^2} - V_0(x) \psi_+ - e^{i(k_+ - k_-)x} V_-(x) \psi_-(x) = 0; \quad (84)$$

$$\psi_-(x) + \frac{h^2}{2m_1} \frac{d^2 \psi_-(x)}{dx^2} - V_0(x) \psi_- - e^{i(k_+ - k_-)x} V_+(x) \psi_+(x) = 0; \quad (85)$$

In this case, the components  $Q$  of the deformation of the  $\alpha$ -helix are also non-zero:

$$Q_+(q) = \frac{2i \sin q}{(1 - \frac{2}{q} V^2 q^2)^{\frac{1}{2}}} \frac{x}{3MN_k} + (k) - (k + q); \quad (86)$$

Substituting this into (58) we find that, for small velocities,

$$V_+ = \frac{2^2}{3w} e^{i(k_+ - k_-)x} \psi_+(x) \psi_-(x); \quad V_- = V_+; \quad (87)$$

The deformational potential  $V_0$  of the totally symmetric distortions is given by

$$V_0(x) = \frac{2^2}{3w} \psi_+(x) \psi_+^2 + \psi_-(x) \psi_-^2; \quad (88)$$

Thus, equations (84) and (85) give us a system of NLSEs:

$$\psi_+(x) + \frac{h^2}{2m_1} \frac{d^2 \psi_+(x)}{dx^2} + \frac{2^2}{3w} \psi_+ \psi_+^2 + 2\psi_+ \psi_-^2 \psi_+(x) = 0 \quad (89)$$

and, equivalently, for  $\psi_-$ .

The general solution of these equations, normalized by the condition (43), is

$$\psi_2 = \frac{1}{\sqrt{2}} e^{i\phi_2} \psi_2; \quad (90)$$

where  $\phi_2$  are arbitrary phases and  $\psi_2$  satisfies the NLSE and is, therefore, given by (67) with

$$\psi_2 = \frac{9}{w(18J + L)}; \quad (91)$$

The total energy of this soliton state at  $V = 0$  is

$$E_2(0) = E_0 - 2J - L \frac{3L^2}{2(18J + L)} - \frac{3^4}{2w^2(18J + L)}; \quad (92)$$

and the soliton mass is

$$M_2 = m_1 + \frac{12^4}{w^2(18J + L)}; \quad (93)$$

Representing the energies of the other two solitons (82) in the form  $E_1(0) = E_b$  with  $E_b = E(k_d)$  being the corresponding bottom of the energy band and

$$= \frac{2^4}{3w^2(18J + L)}; \quad (94)$$

we can write

$$E_2(0) = E_b(0) - \frac{9}{4} = E_1(0) - \frac{5}{4}; \quad (95)$$

Thus, we see that the latter hybrid soliton has the lowest energy.

The distribution of the excitation amongst the chains is given by the probability amplitude:

$$\psi_{jn}^{(n)}(t) = \frac{1}{\sqrt{3}} e^{i(t - \frac{h}{m_1}V(n+j=3) - \frac{+}{2})} \cos(k_d(n+j=3) + \frac{+}{2} + \frac{2}{3}j) \psi_2(n + \frac{j}{3}; t); \quad (96)$$

Therefore,

$$P_{jn} = \int |\psi_{jn}^{(n)}(t)|^2 = \frac{2}{3} \frac{1 + \cos(2k_d(n+j=3) + \frac{+}{2})}{\cosh^2(n + \frac{j}{3} - Vt - \frac{h}{m_1}t)}; \quad (97)$$

Next, we consider the probability distribution of the excitation summed over all the spines of the helix:

$$P_n(t) = \sum_j P_{jn}(t) = \int |\psi_2(n;t)|^2 \left( 1 - \frac{k_d}{3} \cos(2k_d n + \frac{+}{2}) \right) \int |\psi_2(n;t)|^2; \quad (98)$$

for all  $k_d$ , and the total probability of the excitation localisation on a given spine:

$$P_j(t) = \sum_n P_{jn}(t) = \frac{1}{3} \left( 1 - \frac{k_d}{2 \sinh \frac{k_d}{2}} \cos(2k_d Vt - \frac{2}{3}j + \frac{+}{2}) \right); \quad (99)$$

We see from (99) that the probability of the excitation localisation on a given spine is an oscillatory function of time with the period of oscillations given by

$$T = \frac{2\pi}{k_d V}; \quad (100)$$

Thus, the helical symmetry of the system results in the interspine soliton oscillations with a period of oscillations that is determined by the soliton velocity and the quasimomentum value corresponding to the bottom of the energy band (79). These oscillations get mixed up with the oscillations that arise from the influence of the lattice discreteness on the soliton dynamics which leads to the appearance of the Peierls-Nabarro potential. The period of these latter oscillations is also determined by the soliton velocity, (59), as is shown in [19].

## 5 Numerical modeling

For the numerical calculations we consider an  $\alpha$ -helical system of length  $N = 150$  with periodic boundary conditions:

$$f_{j,n+N} = f_{j,n} \quad (101)$$

or, equivalently,

$$f_{1+3N} = f_1; \quad (102)$$

where  $f$  stands for  $\phi$  or  $\psi$  and the index  $l$  enumerates the sites along the polypeptide chain and  $f_{j;n}$  denotes the site number  $n$  in the  $j$ -th hydrogen bond spine ( $j = 1; 2; 3$ ).

It is more convenient, for the numerical simulations, to use the physically more relevant site representation for the  $\psi_{j,n}$  variables and to use  $u_{j,n}$  for the displacements of PGs from the positions of their equilibrium. Here  $u_{j,n}$  are the average displacements of PGs in the state (40) and are related to  $\psi_{j,n}$  by the unitary transformation (36). In these variables the equations (45)–(46) become

$$i\hbar \frac{d\psi_{1,n}}{dt} = E_0 - \psi_{1,n} [J(\psi_{1,n-1} + \psi_{1,n+1}) + L(\psi_{3,n-1} + \psi_{2,n}) + (u_{1,n+1} - u_{1,n-1})\psi_{1,n}]; \quad (103)$$

$$i\hbar \frac{d\psi_{2,n}}{dt} = E_0 - \psi_{2,n} [J(\psi_{2,n-1} + \psi_{2,n+1}) + L(\psi_{1,n} + \psi_{3,n}) + (u_{2,n+1} - u_{2,n-1})\psi_{2,n}]; \quad (104)$$

$$i\hbar \frac{d\psi_{3,n}}{dt} = E_0 - \psi_{3,n} [J(\psi_{3,n-1} + \psi_{3,n+1}) + L(\psi_{2,n} + \psi_{1,n+1}) + (u_{3,n+1} - u_{3,n-1})\psi_{3,n}]; \quad (105)$$

$$M \frac{d^2 u_{j,n}}{dt^2} = -w(2u_{j,n} - u_{j,n-1} - u_{j,n+1}) + (j - j_{n+1})^2 - (j - j_{n-1})^2; \quad j = 1; 2; 3; \quad (106)$$

For  $n = 0$  and  $n = N - 1$  in the expressions above we take the appropriate values of the functions determined by our periodicity conditions.

In our studies we have adopted the following procedure. We have started off with a reasonable field conformation and then used it as an initial excitation to determine a stationary solution of our system of equations (103–106). Having determined this solution numerically, we have kept on modifying it by an adiabatical increase of the wave-vector (thus increasing the velocity of the soliton), and have found for each fixed value of the wave-vector the corresponding stationary solution describing a soliton which propagates along the helix with an increasing non-zero velocity, determined by the gradually increasing values of the carrying wave-vector.

Note that, for an  $\alpha$ -helix, the question about the initial configuration is more important than for a simple chain, because there are three types of solutions, corresponding to the different symmetries. Studying similar problem for a simple linear chain, we had two equivalent approaches of deriving a stationary solution at zero velocity (see, e.g., [19]). Namely, we could start with the system of stationary equations and find the solution by minimizing the energy using some standard procedures. Another approach would use the non-stationary equations which include some dissipation of the energy in the lattice sub-system. Starting with an arbitrary localized initial configuration of an excitation, we would find some time later a stationary solution at zero velocity. Then this configuration would be modified by adding a small carrying wave-vector and would be used as a starting initial condition for the next set of calculations of the system of equations without any dissipation. This would result in a solution moving with a small non-zero velocity. Repeating this procedure further, we would increase the soliton velocity adiabatically till the velocity reaches the maximum value corresponding to the chosen parameters of the chain. This last approach, of using an arbitrary initial configuration, in the case of a helical structure probably cannot describe all possible solutions, since it would always lead to the solution of the lowest energy.

The energy expression can be obtained from (23, 21, 24). In the site representation the total energy is given by

$$E_{\text{tot}} = E_e + E_v + E_{\text{int}}; \quad (107)$$

where

$$\begin{aligned} E_e = & \sum_{n=0}^{N_X-1} \sum_{j=1}^3 \frac{1}{4} X^3 E_{0j} j_{jn}^2 - J \left( j_{jn} j_{jn-1} + j_{jn-1} j_{jn} \right) + \\ & + L \left( j_{1n} j_{3n-1} + j_{3n-1} j_{1n} + j_{2n} j_{1n} + j_{1n} j_{2n} + \right. \\ & \left. + j_{3n} j_{2n} + j_{2n} j_{3n} \right); \end{aligned} \quad (108)$$

$$E_v = \sum_{j=1}^3 \sum_{n=0}^{N_X-1} \frac{M}{2} \left( \frac{du_{jn}}{dt} \right)^2 + \frac{1}{2} w (u_{jn} - u_{jn-1})^2; \quad (109)$$

$$E_{\text{int}} = \sum_{j=1}^3 \sum_{n=0}^{N_X-1} (u_{jn+1} - u_{jn-1}) j j_{jn}^2; \quad (110)$$

In our simulations we have taken the numerical values of the parameters from [12]: i.e.  $L = 12.4 \text{ cm}^{-1}$ ;  $J = 7.8 \text{ cm}^{-1}$ ,  $\mu = 3.4 \cdot 10^{10} \text{ N}$ ,  $w = 19.5 \text{ N/m}$  and  $M = w = 1/a = 0.99 \cdot 10^{13} \text{ s}$ . These parameter values correspond to the Amid-I excitations in  $\alpha$ -helices [15, 20, 12, 5].

In our numerical studies we have also followed the conventions of Scott [12] and so, like him, we have used units in which the energy is measured in units of  $\hbar_a$ , time in units of  $a^{-1}$  and length in units of  $10^{11} \text{ m}$ . In this case the dimensionless computer values of the parameters are

$$\begin{aligned} J_{\text{comp}} = \frac{J}{\hbar_a} &= 0.145; \quad L_{\text{comp}} = 0.231; \quad \text{comp} = \frac{10^{11} \text{ m}}{\hbar_a} = 0.318; \\ w_{\text{comp}} &= \frac{w}{\hbar_a} \frac{10^{22} \text{ m}^2}{\hbar_a} = 1.825; \end{aligned} \quad (111)$$

The results of the numerical simulations are described below.



First, we have started the simulations taking as the initial conditions the function

$$u_{j,1} = 1: \quad (112)$$

with all other values of  $u_{j,n} = 0$  and putting  $u_{j,n} = 0$ : We have then added an extra absorptive term into the equation for  $u_{j,n}$  and performed the simulations until we have reached a stationary state solution. The obtained solution described a well defined solitonic state. Its energy was around -0.55067. In Fig. 2 we present the plots of the  $u_{j,n}$  and  $u_{j,n}$  fields.

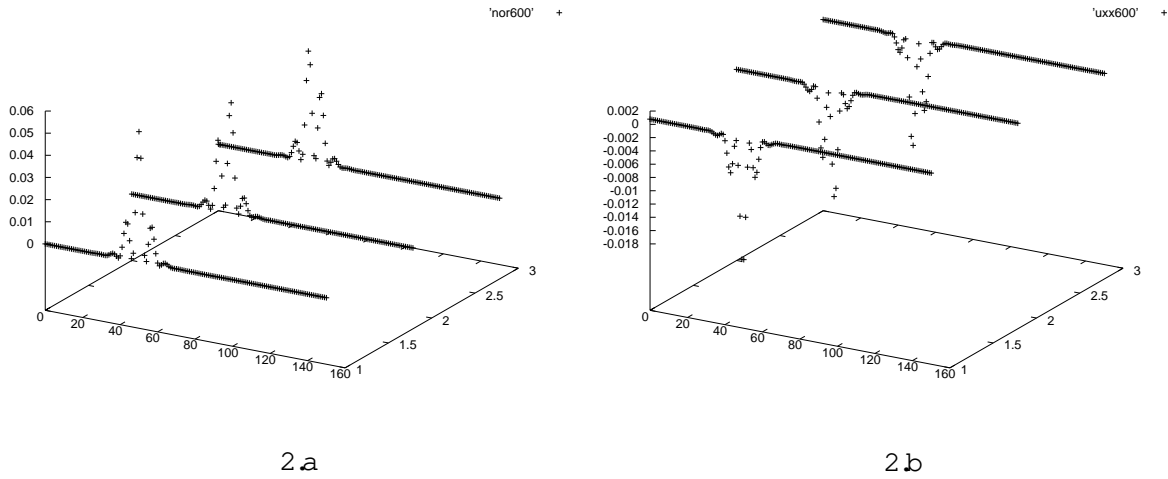


Figure 2: Stationary excitation function (a) and the derivative of the PG's displacement i.e.  $u_{j+1,n} - u_{j,n}$  (b) for the alpha-helix.

We see that this self-trapped state has an inner structure. While the total (summed over all three spines) distribution of the excitation has a single-hump pattern, the distributions in individual spines are modulated in the manner of solutions (97). The same feature can also be seen in Fig.6 of [12]. Thus, we can conclude that our numerical solution, as well as the solution discussed in [12], describes the lowest energy of the hybrid solitons. This view is confirmed also by the numerical estimate of the soliton energy (92). Thus taking our numerical values (111), we get  $E_2(0) = E_0 = -0.55062$  in units of  $\hbar \omega_a$  which coincides with the value determined in our numerical simulations.

Having found stationary solutions, we then changed the functions as follows

$$u_{j,n} \rightarrow u_j e^{in k} \quad \frac{du_{j,n}}{dt} \rightarrow \frac{du_{j,n}}{dt} + (u_{j,n} - u_{j,n-1}) \sin(k) \quad (113)$$

leaving  $u_{j,n}$  unchanged. This had the effect of giving a small speed to the soliton, and the distortion of the chain.

We then performed the simulation over a short period of time. During this time the soliton has been moving and the small disturbance introduced by the nonperfect transfer of momentum to the system has spread itself over the lattice.

We then repeated the whole process several times thus slowly increasing the total  $k$  (in practice we put  $k = 0.1$ ). After every step we evaluated the resultant speed of the soliton. Of course, the whole process suffered by the introduced disturbances; thus gradually it has become more and more difficult to determine this speed. However, we have found that each addition of

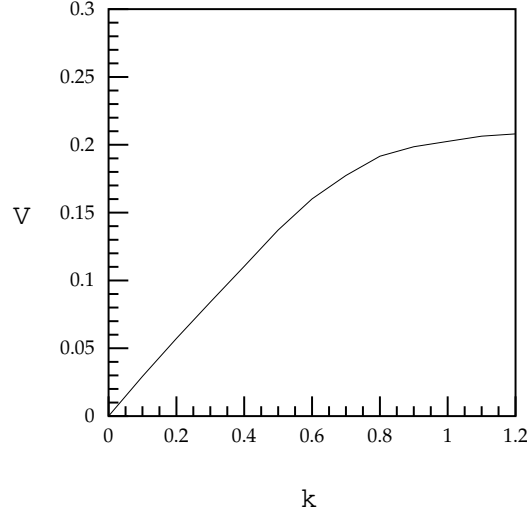


Figure 3: Speed of the hybrid soliton as a function of  $k$ .

momentum increased this speed by a decreasing amount suggesting that there is a maximum speed that the soliton can attain.

In Fig. 3 we present a plot of the resultant speed as a function of the total  $k$  (i.e., the sum of all  $k$ ). We note that the maximum speed appears to be around 0.21. To check that this limit is not an artifact of our procedures, we have performed further simulations in which we modified the steps  $k$  or eliminated the modification of  $\frac{u_{ij}}{dt}$ . We have also performed some simulations with absorption: the configurations were alternatively boosted and then evolved in time but with a small absorption parameter added to the equations. These extra terms absorbed some of the ripples while the boosts were effectively accelerating the solitons. All these procedures produced similar results and we have never managed to get the solitons move faster than with  $v = 0.21$ . The absorptions did decrease the deformations of the  $\phi$ -helix but they did also reduce the velocity of the soliton; hence we do believe that the solitons cannot have larger velocity and that this maximum speed is determined by the maximum allowed group velocity of the excitons.

In Fig. 4 we present the plot of the solutions of (53) for  $E(k)$  with the values of  $J$  and  $L$  given in (111) (we recall that  $v = V = v_a$ ). From Fig. 4 we see that, indeed, the composite soliton cannot have its velocity larger than the maximum group velocity for one of its two components, and for our parameters this velocity is about 0.21. At wavenumber  $k_{cr}$ , which corresponds to the maximum group velocity,  $d^2E(k)/dk^2 = 0$  and at  $k = k_{cr}$  the balance between the nonlinearity and the dispersion breaks down for one of the components and this leads to the decay of the soliton.

The complex (modulated many-hump) and composite (three-spine distributed) structure of the soliton manifests itself distinctly when the soliton is moving and the interspine oscillations take place (99). This is seen very clearly in the oscillations of the probability distribution amplitude for each spine which is shown in Fig. 5. This phenomenon was already noted by Scott in [12]. According to (100), the frequency of these oscillations is determined by  $k_d$  and by the soliton velocity. It follows from (79) that the bottom of the band is attained at  $k_d = 0.42$ .

We have also looked at the other two solitons and tried to make them move. As has already

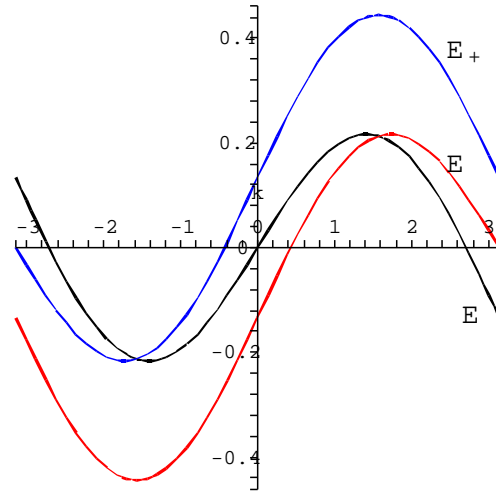


Figure 4: The excitation velocity (53) for  $J = 7.8 \text{ cm}^{-1}$  and  $L = 12.4 \text{ cm}$ .

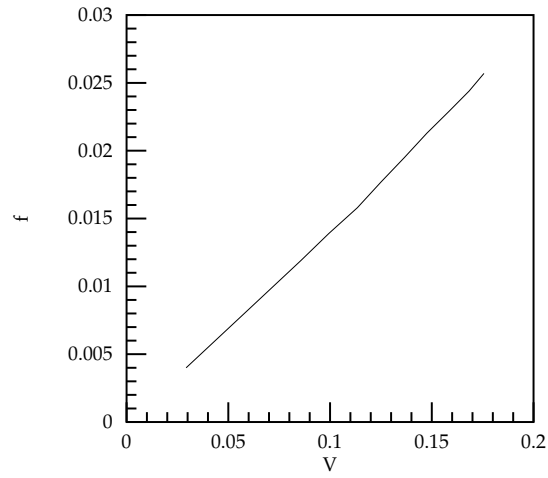


Figure 5: Oscillation frequency of the hybrid soliton as a function of its speed  $V$ .

been mentioned above, an arbitrary initial configuration, in the case of a helical structure always leads to the solution of the lowest energy. But when we take as an initial condition  $j_{jn}$  in the form (71) at  $V = 0$ , we have obtained, as a result of the calculations, stationary solutions and these solutions were very close to those derived in the continuum approximation. The energies of these stationary solutions were +0.171 for  $\alpha = 0$  and 0.54972 for  $\alpha = 2 = 3$  which, again, coincide with the values  $E(0) = E_0$  estimated from (77) and (82). For these states the probability distribution in individual spines  $j^2_{jn}$  shows a one-hump pattern without any modulation (see fig 6). This differentiates these states from the lowest energy composite soliton.

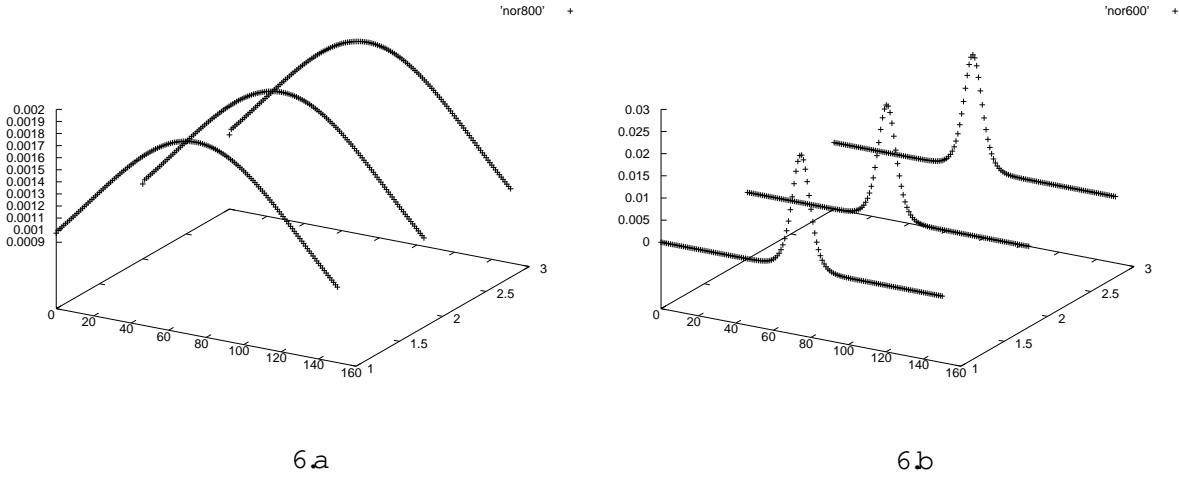


Figure 6: Electron fields for the other solitons - (71) with  $V = 0$ .

We have tried to make these states move. Unfortunately, the perturbations introduced by the discreteness of the lattice and by the inexactness of our procedure led to their instability. This showed itself in the system evolving into the lowest energy (totally symmetric) soliton.

## 6 Conditions for the applicability of the adiabatic approximation

Having found the three types of solutions described in the previous sections a question then arises about the conditions of the applicability of the adiabatic approximation in such a three-spine model.

The Hamiltonian (25) that describes the states of quasiparticles which interact with phonons, does not have an exact solution. The adiabatic approximation describes the soliton-like states of large polarons when the autolocalization, within the region of several lattice sites, takes place. This is one of the three possible approximations which allow us to represent the Hamiltonian (25) as a sum of two terms: the main part,  $H_0$ , and the term,  $H_1$ , which can be considered as a small correction, and, therefore, for which the perturbation theory can be developed. The other two approximations correspond to the almost free quasiparticles and to small polarons. The realization of one or another of these three regimes depends on the relation between the parameters of the system. In general the problem can be investigated in the framework of the variational approach [21, 22, 23]. The ground state diagram for a simple chain with one exciton band and one phonon mode was presented in [21]. This diagram showed the range of values of

the dimensionless coupling constant and of the nonadiabaticity parameter (relation  $h_a = (2J)$ ) for which one or the other regime was realized.

As it has often been mentioned, various properties of the Davydov solitons in  $\alpha$ -helical proteins have been analysed using a single chain model. Although such a model gives good qualitative and sometimes also good quantitative [12] properties of Davydov solitons, the ground state diagram [21, 23] shows that the parameters of the  $\alpha$ -helix applied to a one-chain model, correspond to the state far from the region where the soliton ground states are realized. This is one of the reasons why the estimates by H. Bolterauer [6] and J.W. Schweitzer and J.P. Cottingham [6] of the Davydov soliton life-time, obtained within a different approach but still based on the one-chain model, give very small values.

Here we return to this problem and we assess the conditions of the applicability of the adiabatic approximation for the  $\alpha$ -helix basing our discussion, for simplicity, on the solutions describing solitons at rest. Applying a unitary transformation, the Hamiltonian (25) takes the form  $H = H_{ad} + H_{na}$  where  $H_{ad}$  is diagonal in the new representation and describes the adiabatic states of the exciton (electron)-phonon system. The term  $H_{na}$  is an operator of nonadiabaticity which describes phonon-induced transitions between adiabatic states. Such a transformation was used in [24, 25] and, based on it, a method of partial diagonalization was further developed in [26, 27, 28].

The partial diagonalization shows clearly that the state-vector (40) is an eigenstate of  $H_{ad}$  with the eigenenergy  $E = h + W$  (here  $W$  is the energy of lattice deformation) provided that the functions  $\psi_k$  and  $\varphi_k$  are stationary solutions of equations (45) and (46), i.e.  $H_{ad} j_0 i = E_s j_0 i$ . The virtual excited adiabatic states, for a given chain deformation (52) can be found from the linear equation (45).

If  $H_{na}$  is small it is possible to construct the perturbation series

$$j_i = j_0 i + j_1 i + \dots$$

where  $j_0 i = \psi_i$  is the wavevector (40) of the soliton state in the zero order of the adiabatic approximation and  $j_i i$  is the  $i$ -th correction due to  $H_{na}$ . According to the general theory of perturbations the first correction is given by

$$j_1 i = \frac{Q}{a} H_{na} j_0 i \quad (114)$$

where we have defined

$$\frac{Q}{a} = Q \frac{1}{H_{ad} - E_s} Q$$

and

$$Q = 1 - \sum_{j \neq 0} \frac{j_0 i h_0 j}{E_s - E_j} j_i h_j$$

Note that here  $j_i$  enumerates all adiabatic terms of  $H_{ad}$ ,  $H_{ad} j_i = E_j j_i$ . For the convergence of the perturbation series  $j_i i$  should be proportional to  $\epsilon^i$  with  $\epsilon$  being a small parameter.

The square of the norm of vector  $j_i$  is

$$h j_i = h_0 j_0 i + h_1 j_1 i + \dots = 1 + O(\epsilon^2):$$

Therefore, the applicability of the adiabatic approximation is guaranteed provided that

$$h_1 j_1 i \ll 1: \quad (115)$$

Taking into account (114), we can calculate

$$\langle \psi_1 | \psi_1 \rangle = \langle \psi_0 | \mathcal{H}_{na} \frac{Q}{a^2} \mathcal{H}_{na} | \psi_0 \rangle = \sum \langle \psi_0 | \mathcal{H}_{na} | \psi \rangle \langle \psi | \frac{Q}{a^2} | \psi \rangle \langle \psi | \mathcal{H}_{na} | \psi_0 \rangle \quad (116)$$

$$= \frac{1}{2} \sum f \langle \psi_0 | \mathcal{H}_{na} | \psi \rangle \langle \psi | \mathcal{H}_{na} | \psi_0 \rangle \quad (117)$$

Here we have taken into account the fact that the operator  $\frac{Q}{a^2}$  is diagonal and we have defined

$$f = \frac{1}{2} \langle \psi | \frac{Q}{a^2} | \psi \rangle \quad (118)$$

with  $\epsilon_s$  being the energy gap between the solitonic energy level and the lowest excited one. In (118)

$$= \sum_{\epsilon_s} \langle \psi | \frac{Q}{a^2} | \psi \rangle \quad (119)$$

so that  $\sum_{\epsilon_s} f = 1$ . In (117) the summation does not include  $\epsilon = 0$  because the diagonal matrix elements of the nonadiabaticity operator vanish. Next we observe that

$$\sum f \langle \psi_0 | \mathcal{H}_{na} | \psi \rangle \langle \psi | \mathcal{H}_{na} | \psi_0 \rangle = \sum \langle \psi_0 | \mathcal{H}_{na} | \psi \rangle \langle \psi | \mathcal{H}_{na} | \psi_0 \rangle = \langle \psi_0 | \mathcal{H}_{na}^2 | \psi_0 \rangle \quad (120)$$

Moreover, it is easy to see that

$$\langle \psi_0 | \mathcal{H}_{na}^2 | \psi_0 \rangle = \langle \psi_0 | \mathcal{H}^2 | \psi_0 \rangle - \langle \psi_0 | \mathcal{H} | \psi_0 \rangle^2 = E^2 \quad (121)$$

Thus we can derive some estimates without the partial diagonalization of Hamiltonian (25). In particular, we can calculate  $E^2$  using the soliton wavefunction (40) in the zero order adiabatic approximation. This way we can estimate the soliton life-time in one chain and we get the same result as that obtained by J.W. Schweitzer and J.P. Cottingham [6] who calculated  $E^2$  performing the partial diagonalization, and by Bolterauer [6] who calculated  $E^2$ .

So, the condition of the applicability can be written as

$$\langle \psi_1 | \psi_1 \rangle \ll \frac{E^2}{2} \ll 1 \quad (122)$$

Calculation of  $E^2$  gives us

$$E^2 = \frac{1}{2} A \sum_{\mathbf{q}} \langle \psi | \frac{Q}{a^2} | \psi \rangle \quad (123)$$

where

$$A = \sum_{\mathbf{q}} \frac{4h^2 \sin^2 \mathbf{q}}{3M N |\mathbf{q}|} = \frac{16h^2 a^2}{3w} \quad (124)$$

Taking into account (52) we can rewrite (123) in the form

$$E^2 = \sum_{\mathbf{q}} \frac{2h^2 \sin^2 \mathbf{q}}{3M N |\mathbf{q}|} \sum_{\mathbf{k}} \langle \psi | \mathcal{H}_{na} | \mathbf{k} \rangle \langle \mathbf{k} + \mathbf{q} | \mathcal{H}_{na} | \psi \rangle$$

which corresponds to Bolterauer's [6] expression after the transformation to the site representation.

For symmetrical solitons  $Q_+(q) = Q_-(q) = 0$  and

$$Q_0(q) = \frac{2i \sin q}{!_q 3M N} \sum_k^X (k+q) \quad (k) = \frac{2i \sin q}{!_q 3M N} \sum_{N=2}^Z e^{iqx} \int_{N=2}^Z (x) f dx; \quad (125)$$

where

$$\sum_{N=2}^Z e^{iqx} \int_{N=2}^Z (x) f dx = \frac{q}{2 \sinh \frac{q}{2}}; \quad (126)$$

Therefore,

$$E_1^2 = \frac{8h_a^2}{3w} (1 - \frac{18}{2} \cdot 2): \quad (127)$$

For the hybrid soliton we have

$$Q_0(q) = \frac{2i \sin q}{!_q 3M N} \sum_{N=2}^Z e^{iqx} \int_{N=2}^Z (x) f dx + \sum_{N=2}^Z e^{iqx} \int_{N=2}^Z (x) f dx \quad (128)$$

and

$$Q_+(q) = Q_-(q) = \sum_{N=2}^Z e^{i(q+2k_d)x} \int_{N=2}^Z (x)' \cdot (x) dx; \quad (129)$$

$$E_2^2 = \frac{8h_a^2}{3w} (1 - \frac{72}{2} \cdot 2 - \frac{6}{6} \cdot 2 \sin k_d \cos^2 k_d): \quad (130)$$

In the one-dimensional case, the soliton level (121) is a single bound level in the lattice deformation potential. Excited adiabatic states belong to the quasi-continuum spectrum with eigenenergy  $(k) = \frac{\hbar^2 k^2}{2m}$  which is separated from the soliton level by a gap  $= \frac{\hbar^2 \cdot 2}{2m}$ . Therefore, we can estimate (119) as

$$= \frac{n}{N} \sum_k^X \frac{4}{(2 + k^2)^2} = \frac{n}{4}; \quad (131)$$

where  $n = 1$  for the totally symmetric soliton, and  $n = 2$  for the hybrid soliton since, in this case, there are two degenerate bands.

Finally, we have the conditions for the realization of the soliton-like states:

$$_0 = \frac{s}{2C_0 w} \frac{p}{h_a (9J + L)} < 1 \quad (132)$$

for the total symmetric soliton, and

$$_1 = \frac{s}{2C_1} \frac{2}{3} \frac{3}{2} \frac{p}{w} \frac{h_a (18J + L)}{2} < 1 \quad (133)$$

for the composite soliton, respectively. Here

$$C_0 = 1 - \frac{18}{2} \cdot 2_0$$

and

$$C_1 = 1 - \frac{1}{6} k_d \cdot 2 - \frac{72}{2} \cdot 2_2$$

where we have assumed that  $k_d$  and  $< 1$ .

Note that the condition (132) coincides with the condition which can be obtained in the partial diagonalization scheme for the one chain model [27, 26]. This condition indicates that solitons can exist in soft enough chains and at a strong enough exciton (electron)-phonon coupling they are stable against quantum fluctuations. The relation (132) is the inverse of the condition for the weak coupling regime.

The numerical values of the parameters for the  $\alpha$ -helix are:  $J = 1.55 \cdot 10^{22}$  Joule,  $L = 2.46 \cdot 10^{22}$  Joule,  $\kappa = 35 \cdot 62 \cdot 10^2$  N,  $w_H = 13 \cdot 19.5$  N/m. We can take  $\tau_a = 10^{-13}$  s. For these parameters we get  $\tau_0 = 2.3 \cdot 11$  for the total symmetric soliton, which corresponds to the one-band model. Therefore, in this case, the adiabatic approximation is not valid, and, consequently, the soliton is destroyed by quantum fluctuations. The corresponding estimates for the composite soliton give the value  $\tau_1 \approx 1$ . For instance, for  $\kappa = 62 \cdot 10^2$  N and  $w_H = 14.6$  N/m we get  $\tau_2 = 0.87$ , and, therefore, the perturbation series converges. It is worth adding here that the larger values of the coupling and the condition that the chains are softer strengthen the condition for this type of soliton solution to exist.

## 7 Conclusions

As we have mentioned above, the main aims of this paper were the study of the soliton states in  $\alpha$ -helical proteins taking into account their helicity structure and the understanding of the origin of the inter-spine oscillations observed numerically by Scott in [12]. The soliton states in  $\alpha$ -helical proteins are described by a system of nonlinear equations (103-106). In our study we have restricted the Hamiltonian of amide excitations to two main terms, namely, those that describe the intra- and inter-spine interactions, while Scott considered ten additional terms of long-range resonance interactions. Our results broadly reproduce the results of Scott. However, there are also some differences, which we summarize below.

The velocity of the soliton propagation in the numerical calculations carried out by Scott in [12], was reported as  $V = \frac{3}{8} v_a$ , while our results give the maximum value  $V = 0.21 v_a$ . This is due to the fact that in [12] further terms of the resonance interaction of Amide-I vibrations were included, which increase the width of the exciton bands and, therefore, increase the exciton group velocity. The additional terms in the Hamiltonian also change the corresponding value of  $k_d$ , but, probably, this change is less significant than the change of the maximum group velocity. Nevertheless, our formula (100) of the period of oscillations for the values  $\tau_a = 10^{-13}$  s and  $k_d = 0.42$  for the  $\alpha$ -helix at  $V = \frac{3}{8} v_a$ , gives  $T = 1.995 \cdot 10^{12}$  s, which practically coincides with the value obtained by Scott,  $T_{\text{comp}} = 2 \cdot 10^{12}$  s.

Our analytical study and the numerical simulations elucidate the conditions for the existence of various types of soliton solutions: single-band and mixed two-band solitons. The entangled two-band (hybrid) solitons break spontaneously the translational and rotational symmetries, and possess the lowest energy. Single-band solutions break only the translational symmetry and preserve the rotational symmetry. Single-band solitons turn out to be dynamically unstable: once initially formed, they decay rapidly while propagating. There are two main reasons for this, which arise from the helical structure of the system, namely, the absence of the forbidden gap in the energy spectrum (see Fig. 1) and the Umklapp processes. The absence of the energy gap allows the transition to the lowest energy state via the interactions with low-energy phonons. The helical symmetry leads to the relation  $\epsilon(k - 2) = \epsilon_1(k)$ , i.e., the mixing of single-band states takes place, and, as a result, the single-band solutions decay. This is the reason why given any initial condition the excitation localises into the state which corresponds to the lowest



energy, i.e., to the entangled soliton. In particular, this was the case observed in [12]. We have managed to observe such solitons due to the very special choices of the initial excitations which were very close to the expression for the stationary single-band soliton at rest.

It is also worth comparing this type of solution in a helical system with those in a three-spine model without helical symmetry. In the latter case there is a forbidden gap in the energy spectrum between the two degenerate bands and the third band. As a result, the initial excitation with the energy above the forbidden gap, is self-trapped in a single-band soliton state. The totally symmetric soliton predicted analytically in [8, 9] was observed numerically in [10, 11]. Such a soliton in a chain without helical symmetry can be destroyed only if a large amount of energy is supplied to the system. Therefore, these single-band localised solutions are much more stable dynamically than single-band solitons in chains with helical structures. This constitutes a qualitative difference between the three-chain system with an helical symmetry and the one without it.

The important question about the existence of Davydov solitons in  $\alpha$ -helical proteins remains open. Unlike the case of conducting polymers, for which there is reliable experimental evidence for the soliton (large polaron and bipolaron) existence, such data are absent for polypeptides. The answer to this question is related to the applicability of the adiabatic approximation, which is determined by the numerical values of the parameters of a given system. Solitons can exist in protein macromolecules provided their parameters satisfy the condition of the adiabatic approximation. Note, e.g., that the spring constant for the hydrogen bond  $w_H$  was determined in [20] to be 21 N/m. Scott [12], who takes into account that the hydrogen bonds in the  $\alpha$ -helix are  $22^\circ$  oriented, uses the value 19.5 N/m. But as it has been shown above, the effective value is  $w = \cos^2 \theta w_H$  where  $\theta$  is determined in (19). For the parameters of the  $\alpha$ -helix  $a = 5.4\text{\AA}$  and  $r = 1.7\text{\AA}$  we get  $\cos^2 \theta = 0.9$  and, therefore,  $w = 17.05\text{ N/m}$ . Thus, the geometrical factor helps to satisfy the condition for the existence of a soliton.

As we have seen above, the generally accepted parameters for Amide-I excitation do not favour the existence of single-band solitons. On the other hand, they are proper for the existence of the entangled soliton states, although the nonadiabatic corrections are also important and ought to be taken into account. Thus, the one-chain model can give good qualitative results, but conclusions concerning the existence and stability of soliton states, based on numerical calculations within such an oversimplified model, may not always be correct. Of course, our estimates are relatively rough, and the method of partial diagonalization of the Hamiltonian would provide better results. Its generalization to systems involving three-chain macromolecules can face the problem of the applicability of the long-wave approximation. In such cases the partial diagonalization method developed for discrete models by Clogston et al. [28] may turn out to be useful. Moreover, the variational methods can give better results (see, e.g., [29, 22, 21, 23]) for the crossover states when the perturbation scheme parameter is not very small.

## 8 Acknowledgement

This work has been supported by a Royal Society grant.

## References

- [1] Davydov A S 1973 J. Theor. Biol. 38 559-569.
- [2] Davydov A S, Kislukha N I 1973 Phys. Stat. Sol. (b) 59 465-470.
- [3] Davydov A S, Kislukha N I 1976 Zh. Eksper. Theor. Fiz 71 1090.
- [4] Davydov A S, Solitons in Molecular Systems (Dordrecht: Reidel) 1985.
- [5] Scott A C 1992 Phys. Rep. 217 1.
- [6] Davydov's Soliton Revisited Christiansen P L. and Scott A C. eds. (New York: Plenum) 1990.
- [7] Davydov A S, Suprun A D 1974 Ukr. J. Phys. 19 44-50.
- [8] Davydov A S., Eremko A A., Sergienko A I. Ukr. J. Phys. 1978, 23, No 6, 983-993
- [9] Eremko A A., Sergienko A I. Ukr. J. Phys. 1980, 25, No 12, 2013-2020.
- [10] Hym an J M, McLaughlin D W and Scott A C 1981 Physica 3D 23-44
- [11] D. Hennig Phys. Rev. B, 2002, 65, No 17, 174302.
- [12] Scott A C. Phys. Rev. 1982, A 26., No 1, p. 578-595.
- [13] Fedyanin V K., Yakushevich L V. Int. Journ. Quant. Chem., 1982, 21. No 6, p. 1019-1028.
- [14] Lomdahl P S., McNeil L., Scott A C., Stoneham M E., Webb S J. Phys. Lett., 1982, A 92., N 4, p. 207-210.
- [15] Nevskaya N A, Chirgadze Yu N 1976 Biopolymers 15 637.
- [16] V A. Kuprievich, Physica, D 14, 395 (1985).
- [17] A A. Vakhnenko, and Yu B. Gaididei, Teor. Mat. Fiz., 68, 350 (1986).
- [18] O O. Vakhnenko, and V O. Vakhnenko, Phys. Lett., A 196, 307 (1995).
- [19] L. Brizhik, L. Cruzeiro-Hansson, A. Eremko, Yu. O. Khovska. Phys. Rev., B 61 2002, 1129-1141.
- [20] V A. Kuprievich and Z G. Kudrinskaja, preprints ITP-82-63E, ITP-82-64E, Institute for Theoretical Physics, Kiev (1982).
- [21] Brizhik L S, Eremko A A, La Magna A and Pucci R 1995 Phys. Lett. A 205 90.
- [22] Brizhik L S, Eremko A A and La Magna A 1995 Phys. Lett. A 200 213.
- [23] L. Brizhik, A. Eremko 2000 Synthetic Metals 109 117-121
- [24] A A. Eremko 1984 Dokl. Akad. Nauk UkrSSR, Ser. A, No. 3, 52-55
- [25] A A. Eremko, Yu B. Gaididei, A A. Vakhnenko 1985 Phys. Stat. Sol. (b) 127 703-713
- [26] L. S. Brizhik, A A. Eremko 1995 Physica D 81 295-304
- [27] J P. Cottingham, J W. Schweitzer 1989 Phys. Rev. Lett. 62 1792; J W. Schweitzer Phys. Rev. A 45 8914
- [28] A M. Clogston, H K. McDowell, P. Tsai, J. Hanssen 1998 Phys. Rev. E 58 6407-6417
- [29] D W. Brown, Z. Ivic 1989 Phys. Rev. B 40 9876.